Pages 135-161

ANALYSIS AND TESTING OF THE STEADY-STATE TURNING OF MULTIAXLE TRUCKS

Christopher Winkler
University of Michigan Transportation Research Institute

John Aurell
Volvo Truck Corporation

ABSTRACT

The International Standards Organization (ISO) is currently involved in an effort to develop a standard test procedure for evaluating the steady-state turning behavior of heavy vehicles.[1] In the course of developing this standard, a new analysis has evolved which expands the basic understanding of the steady-state turning of all motor vehicles.

The established, simplified analyses of steady-state turning are based on a simple vehicle model in which lateral acceleration is the only motion variable that affects tire slip angles. The new analysis examines a more complex vehicle whose slip angles depend on lateral acceleration plus another motion variable. Basic differences in the steady-state turning behavior of simple and complex vehicles are explained using the handling diagram. It is shown that the complex vehicle can be represented as a simple vehicle with an equivalent wheelbase. Trucks with multiple, nonsteering rear axles are one example of the complex vehicle. An analysis specific to such trucks is presented as is a physical interpretation of the equivalent wheelbase of trucks. Results from simulated and actual track tests which confirm this analysis are presented.

INTRODUCTION

The steady-state handling performance of the pneumatic-tired vehicle has been well understood for some time. While many papers on the subject appear in the literature, Pacejka presented an excellent review of the state-of-the-art understanding in a series of three papers in 1973 [1,2,3] [2] The more germane points of these papers are reviewed herein, but the reader is urged to become familiar with these papers before proceeding.

Pacejka's work, as, indeed, virtually all similar analyses in the literature, concentrates on (what will be called herein) the *simple vehicle* whose steady-state turning behavior is of the form:

$$\delta - \ell/R = \alpha_r - \alpha_f = f(a_y) \quad (1)$$

where
- α_i i = f,r, are the front- and rear-tire slip angles, respectively,
- δ is the steer angle of the front tires,
- ℓ is the wheelbase,
- a_y is lateral acceleration, which, for small angles, is equal to V^2/gR,[3,4]
- R is turn radius, and
- g is the gravitational constant.

In the third paper of the series, however, Pacejka briefly considered (what will be called herein) a more *complex vehicle* for which the difference between front and rear slip angles is a function of lateral acceleration *and* an additional motion variable (velocity and/or path curvature in some combination other than lateral acceleration). As an example of the kind of mechanisms that can lead to complex vehicles, Pacejka noted that the component of front tire side force

acting laterally to the vehicle declines significantly for large steer angles. (That is, the actual lateral component is [F_{yf} cos(δ)]). If this mechanism is included in the handling analysis, then handling properties become a function of steer angle, and the far right side of equation 1 can be reformulated as a function of lateral acceleration *and* velocity. There are numerous other mechanisms that result in this more complex form of the steady-state handling equation for passenger cars, but all of these tend to be of second-order importance.

Commercial trucks, on the other hand, often have a strong, first-order complex influence deriving from the use of multiple, nonsteering rear axles and dual tires. Vehicles that are so equipped develop substantial tire slip angles as a direct result of path curvature, even when traveling at very low speeds, i.e., at near-zero lateral acceleration. (So-called *tire scrub* during tight turns in the parking lot is well known to all truckers.) For these vehicles, then, the far right side of equation 1 is formulated as a function of lateral acceleration *and* path curvature.

This paper will review new analyses of the steady-state turning of complex vehicles in general and of the commercial truck in particular. These analyses reveal new insights into the understeer/oversteer qualities of all motor vehicles [4]. Results from vehicle simulation and from full-scale testing that confirm these analyses will then be presented.

REVIEW OF THE STEADY-STATE TURNING OF THE SIMPLE VEHICLE AND OF THE HANDLING DIAGRAM

The classic analyses of the simple vehicle, including Pacejka's, are based on the highly simplified, *bicycle model* of **figure 1** [1] [5] From the geometry of the figure, assuming small angles (an assumption that is made for this and all similar developments in this paper), and with the principles of statics and the definition of tire cornering stiffness (the change in tire lateral force with slip angle at a slip angle of zero), the following holds for small angles:

$$\delta - \ell/R = \alpha_r - \alpha_f = K a_y \ , \qquad (2)$$

where $$K = F_{zf}/C_{\alpha f} - F_{zr}/C_{\alpha r} \ , \qquad (3)$$

and $C_{\alpha i}$ i = f,r, are the sums of the cornering stiffnesses of all front tires and of all rear tires, respectively,[6]

F_{zi} i = f,r, are the sums of the vertical loads on all front tires and on all rear tires, respectively,[6]

K is the compliance factor of the vehicle,

V is the speed of travel.

Equation 3 is the so called *handling equation* of the simple, linear vehicle. Pacejka showed that there is an analogous equation for the nonlinear case of the simple vehicle [2]. In that equation, the constant K is replaced by the function K'(a_y) and the variables δ, R, and a_y are replaced by their respective perturbations. The compliance factor becomes

$$K'(a_y) + F_{zf}/\phi_f - F_{zr}/\phi_r \ , \qquad (4)$$

where $$\phi_i = dF_{yi}/d\alpha_i \qquad \text{for } i = f, r \ , \qquad (5)$$

and the values of ϕ_f and ϕ_r vary with a_y. The handling qualities revealed by equation 2 thus hold for the linear vehicle in general or for the nonlinear vehicle near a particular operating point. (Note that K and $C_{\alpha i}$ are the special cases of K' and ϕ_i, respectively, for the case of linear tires.)

Equation 2 is the basis for the definition of the understeer gradient. The Society of Automotive Engineers (SAE) and the International Standards Organization (ISO) define this gradient as the difference in the gradient of steer angle, δ, and the gradient of path curvature normalized by the vehicle's wheelbase, ℓ/R (both gradients with respect to a_y) [5,6].[7, 8] For these simple vehicles, it can be shown that the understeer gradient is equal to the value of K'. That is,

$$d\delta/da_y - d(\ell/R)/da_y = d(\delta - \ell/R)/da_y = K' \ . \qquad (6)$$

When this gradient is equal to zero, the vehicle is said to be *neutral steer*. When it is positive, the vehicle is said to be *understeer*, and when it is negative, the vehicle is said to be *oversteer*.

Pacejka showed that stable, steady-state turning requires that[9]

$$\partial\delta/\partial\ell/R > 0 , \tag{7}$$

and that instability can occur only when the understeer gradient (i.e., the value of K') is negative and the vehicle is operating above the *critical velocity* [2]:

$$V_{cr} = (-g\ell/K')^{1/2} . \tag{8}$$

As an aid to explaining his analyses, Pacejka created the *handling diagram* [1]. The handling diagram is a two-dimensional plot with acceleration on the ordinate and radians on the abscissa. The handling equation (equation 2 or its nonlinear equivalent) *and* lines of constant velocity (V-lines) *and* lines of constant, normalized path curvature (ℓ/R-lines) are all plotted on this plane. **Figure 2** presents several versions of such a handling diagram. Note that ($\delta - \ell/R$) is positive to the left (the handling curves), but that ℓ/R is positive to the right (the V- and ℓ/R-lines).

As shown in the figure, the relationships between steer angle, normalized path curvature, and velocity are all visually apparent from the diagram as are the fundamental handling qualities described above. That is:

- Since the handling curve is a plot of a_y versus $\delta - \ell/R$, the slope of the handling curve, $da_y/d(\delta - \ell/R)$, indicates the understeer/oversteer quality of the vehicle. A positive slope (up and to the left) indicates understeer, a vertical slope indicates neutral steer, and a negative slope (up and to the right) indicates oversteer.

- Critical velocity at an operating point where the vehicle is oversteer corresponds to the velocity of the V-line that is parallel to the handling curve at that operating point. At the stability/instability boundary, $d(\delta - \ell/R)/da_y = -g\ell/V^2$) By the relationship $a_y = V^2/gR$, the inverse of the slope of a V-line is $g\ell/V^2$. Thus, at this boundary, the operating line and the V-line for critical velocity are parallel.

STEADY-STATE TURNING OF COMPLEX VEHICLES

By the definition given in the introduction to this paper, the handling equation for a complex vehicle may be expressed in either of the following general forms:

$$\delta - \ell/R = \alpha_r - \alpha_f = f_1(a_y,V) , \tag{9a}$$

$$\delta - \ell/R = \alpha_r - \alpha_f = f_2(a_y,1/R) . \tag{9b}$$

Since complex effects may be fundamentally related to either path curvature or to velocity, either equation 9a or equation 9b may be more desirable for intuitive understanding (and perhaps, for related dynamic analyses). Bear in mind, however, that for steady-state performance, there is always a direct transformation between f_1 and f_2, such that the two forms of equation 9 may be alternate formulations of the same vehicle, not necessarily of different types of vehicles.

Consider the handling diagram for a complex vehicle as shown in **figure 3**.[10] The steady-state handling performance of the vehicle is presented as a family of handling curves. Each curve represents the steady-state handling equation for one specified velocity. These individual handling curves are called V-handling curves. The set of V-handling curves map the handling properties of the vehicle over the range of interest.

Like the handling diagram for the simple vehicle, this more complex diagram shows the relationships between velocity, steer angle, and normalized path curvature. However, since the individual handling curves represent behavior at one velocity only, a given V-handling curve can only be directly compared to its one, corresponding V-line. Required steer angle is represented by the horizontal distance between a V-handling curve and its V-line. Normalized path curvature is shown by the abscissa value of the V-line at the selected acceleration.
The basic criterion for stability (equation 7) and the concept of critical velocity (equation 8) remain valid for the more general case of the complex vehicle.[11] Therefore, as was the case with the simple vehicle, the onset of instability can be determined by comparing the V-

handling curves with the V-lines. (This is demonstrated more formally in [4].) But again, the only legitimate comparison is between a specific V-handling curve and the V-line for the same velocity. Where these two lines are parallel, the vehicle is operating at the stability boundary. As shown in **figure 4**, the locus of these critical conditions identifies the boundary between stable and unstable operating regions.[12] Like the simple vehicle, the complex vehicle can only be unstable when its V-handling curve has a negative slope. However, it is not true (as it is for the simple vehicle) that a negative slope of a V-handling curve *necessarily* implies that this velocity is critical at some level of lateral acceleration. For example, the 60-kph handling curve of figure 4 takes on a negative slope, but nowhere is it parallel to the 60-kph V-line.

Path-curvature information is less clear in figure 3 than it was in the handling diagram of the simple vehicle. A V-handling curve represents conditions of constant velocity, not constant radius. Thus, none of the V-handling curves can be compared, one-to-one, with ℓ/R-lines as could be done for the single handling curve of a simple vehicle.

This suggests that R-handling curves might also be plotted for the complex vehicle. R-handling curves may be constructed directly from the set of V-handling curves. That is, each value of V and a_y implies a specific value of R. R-handling curves are constructed by connecting points of constant R.

Figure 5 is the handling diagram for the complex vehicle with R-handling curves superimposed on the V-handling curves of figure 3. Required steering angles and velocities can now be determined for a vehicle operating on a curve of specific radius by comparing the R-handling curve with its (one-and-only) ℓ/R-line. Note also, that the simultaneous presentation of V- and R-handling curves is graphical confirmation of the earlier assertion that equation 9a (represented by the V-handling curves) and equation 9b (represented by the R-handling curves) can be alternate formulations of the same vehicle.

The appearance of figure 5 immediately raises a difficult question about the nature of understeer for complex vehicles. The figure demonstrates graphically that the expression $d(\delta - \ell/R)/da_y$ is multivalued at every operating point of the complex vehicle. That is, the grid-like nature of the V- and R-handling curves indicates that, within the operating range, there is a valid operating point for the vehicle at every point on the a_y versus $(\delta - \ell/R)$ plane. As a corollary, depending on a specified "test condition" (a specified constraint on the relationship between V and ℓ/R), one can imagine "leaving" a given operating point in any direction on the plane of the handling diagram. Thus, at each operating point, $d(\delta - \ell/R)/da_y$ may take on *any* value depending on the specified constraint between velocity and radius. It seems then, that without a specific constraint, the vehicle cannot be said to be understeer, neutral steer, or oversteer—or it can be said to be all three at once.

Two obvious candidates for the necessary constraint are, of course, constant velocity and constant radius. Under these conditions, $d(\delta - \ell/R)/da_y|_{V=Vc}$ (the gradient at constant velocity, V_c) and $d(\delta - \ell/R)/da_y|_{R=Rc}$ (the gradient at constant radius, R_c) take on singular values. The first of these, of course, is reflected in the slope of the V-handling curves and the second in the slope of the R-handling curves. But at every operating point where a V-handling curve is vertical, there is an R-handling curve that is not vertical, and vice versa. Is the vehicle neutral steer and not neutral steer at the same operating point, or should one of these gradients be favored as the true understeer gradient?

Justification for viewing the gradient *at constant radius* as the understeer gradient is rooted in notions perhaps as significant to closed-loop performance as to open-loop performance. This condition embodies the physical property of simple-vehicle neutral steer most readily identified by the driver. When this gradient is zero, $\partial\delta/\partial V = 0$ [4]. This is the mathematical expression of the physical fact that, given the choice of a specific steer angle by the driver, the vehicle will follow the same arc independent of forward speed. Stated another, more formal way, $\partial\delta/\partial V = 0$ is the operating condition at which the two primary driver-control inputs, steering and throttle, are mechanically decoupled and become "pure" (independent) path and velocity controllers, respectively. Further, when the vehicle is understeer relative to this criterion, more aggressive (faster) cornering requires *more* steering input while the opposite is true for the vehicle that is oversteer relative to this criterion.

The link between the traditional notion of neutral steer for the simple vehicle and the gradient *at constant velocity* for the complex vehicle is clear in a mathematical sense and is related to the open-loop stability of the vehicle. That is, whenever the slope of the V-handling curve is vertical, $\partial\delta/\partial\ell/R = 1$ (which is also true of neutral steer condition for the simple vehicle [1])

[4]. Therefore, at this condition, the requirement for stability, $\partial\delta/\partial\ell/R > 0$ is insured. But $\partial\delta/\partial\ell/R > 0$ is insured just as well by $\partial\delta/\partial\ell/R = 1, 1/2, 2, 10$ or any other, fairly large, positive number. The peculiar positive value of unity does not seem all that significant.

This question as to the "proper" understeer gradient can be resolved, however, by replacing the actual wheelbase, ℓ, with an *equivalent wheelbase*, ℓ_e [4].

In physical terms, in the vicinity of any given operating point, the steady-state turning behavior of the complex vehicle is the same as the steady-state turning behavior of a simple vehicle with a wheelbase of ℓ_e (and, of course, equivalent tires and mass distribution).

Then in mathematical terms, the "proper" value of ℓ_e is the value which results in $d(\delta - \ell_e/R)/da_y|_{V=Vc} = (\delta - \ell_e/R)/da_y|_{R=Rc}$. That is, for any given operating point, their is a constant, ℓ_e, which, when used to normalize path curvature, results in the equality of the constant-radius and constant-velocity gradients in the vicinity of that operating point.

If a handling diagram for a complex vehicle is prepared with the abscissa based on ℓ_e rather than on ℓ, the V- and R-handling curves will be superimposed and will appear as a single curve in the vicinity of the operating point for which ℓ_e was defined. Further, *the understeer gradient* implied by the slope of this single curve *is the same as the gradient at constant radius* based on the actual wheelbase (or for that matter, any other constant). (See reference [4] for the mathematical developments underlying these statements.)

These facts, when combined with the earlier observation that the slope of the V-handling curves (based on ℓ_e, or for that matter, any other constant [4]) are indicative of critical velocity and, therefore, of stable or unstable turning, lead to the following principal observations:

- *Stability gradient* is the appropriate name for the quantity $d(\delta - \ell_e/R)/da_y|_{V=Vc}$, i.e., the gradient at constant velocity. At the open-loop stability boundary (i.e., at $\partial\delta/\partial(\ell_e/R) = 0$) this gradient, $d(\delta - \ell_e/R)/da_y|_{V=Vc}$, is equal to $-g\ell_e/V_c^2$ and thereby identifies the critical velocity. This is true for any arbitrary, positive, and finite value of the constant ℓ_e.

- *Understeer gradient* is the appropriate name for the quantity $d(\delta - \ell_e/R)/da_y|_{R=Rc}$, i.e., the gradient at constant radius. At the operating condition at which path curvature depends only on steer angle and not on speed (i.e., *neutral steer*, or where $\partial\delta/\partial V = 0$), this gradient, $d(\delta - \ell_e/R)/da_y|_{R=Rc}$, equals zero. Further, this condition marks the boundary between the region in which steering must be increased in order to maintain path as speed increases (understeer) and the region in which steering must be decreased to maintain path as speed increases (oversteer). This is true for any arbitrary, positive, and finite value of the constant ℓ_e.

- *Equivalent wheelbase* is the value of ℓ_e which results in equality of the stability gradient and the understeer gradient (i.e., $d(\delta - \ell_e/R)/da_y|_{V=Vc} = d(\delta - \ell_e/R)/da_y|_{R=Rc}$) and the related simultaneous occurrence of $\partial\delta/\partial(\ell_e/R) = 1$ and $\partial\delta/\partial V = 0$ [4]. Equivalent wheelbase is an inherently significant vehicle parameter in that it is the characteristic longitudinal dimension of the vehicle which, when used to normalize path curvature, allows its steady-state turning behavior to be interpreted in a clear and simple manner (i.e., the superposition of the R-handling and V-handling curves).

STEADY-STATE TURNING OF THE COMMERCIAL TRUCK

Simplified Analysis

In 1978, a linear analysis of the steady-state cornering performance of the commercial truck appeared in the literature [10]. This analysis was based on a bicycle model of the type shown in **figure 6**. The analysis included the influence of dual tires as well as multiple, nonsteering axles. In the appendix of that paper, a general solution for the steady-state handling equation was developed for vehicles like that of figure 6, but with any number of axles, n, of which N = n – 1 are nonsteering, rear axles. This general solution is quite complicated, but when it is assumed that all of the N rear axles are (1) subject to equal vertical loading and (2) equipped with similar, linear tires, the general solution was shown to simplify to

$$\delta - \frac{\ell}{R} = \frac{1}{\ell R}\left(\frac{\sum_{i=2}^{n}\Delta_i^2}{N} + D^2\frac{C_{sr}}{C_{\alpha r}}\right)\left(1 + \frac{C_{\alpha r}}{C_{\alpha f}}\right) + a_y\left(\frac{F_{zf}}{C_{\alpha f}} - \frac{F_{zr}}{C_{\alpha r}}\right) \qquad (10)$$

where Δ_i i=2,n, is the longitudinal distance from the aft end of ℓ to the i^{th} axle,
C_{sr} is the sum of the longitudinal stiffnesses of all rear tires,
D is the lateral spacing of dual tires,

and the aft end of the wheelbase, ℓ, is the geometric center of the group of rear axles.

For simplicity, it is also assumed that the influence of dual tires is small relative to the influence of multiple, nonsteering axles. That is,

$$\left| D^2 \frac{C_{sr}}{C_{\alpha r}} \right| << \frac{\sum_{i=2}^{n} \Delta_i^2}{N} \tag{11}$$

Further, to simplify notation, the *tandem factor* is defined as

$$T = \frac{\sum_{i=2}^{n} \Delta_i^2}{N}, \tag{12}$$

and the ratio of rear-to-front cornering stiffnesses is expressed as

$$C_{\alpha r/f} = C_{\alpha r}/C_{\alpha f} . \tag{13}$$

Inserting equations 11 through 13 plus K, as defined by equation 3, into equation 10 yields:

$$\delta - \frac{\ell}{R} = \frac{T}{\ell R}\left[1 + C_{\alpha r/f}\right] + a_y K . \tag{14}$$

Equation 14 (and, for that matter, equation 10) is clearly of the form of equation 9b. That is, the right side of the equation is of the form, $f_2(a_y,1/R)$. As with the simple vehicle, the right side of the handling equation includes the familiar compliance factor multiplied by a_y, but a new term composed of a function of vehicle properties multiplied by path curvature has appeared. Thus, the linear truck with multiple, nonsteering axles is a complex vehicle.

The equivalent wheelbase of this truck can be determined directly from equation 14 by rearranging it into the following form.

$$\delta - = a_y K , \tag{15}$$

where $$\ell_e = \ell \left[1 + T/\ell^2 \left(1 + C_{\alpha r/f}\right)\right] . \tag{16}$$

The similarity between equation 2 (the handling equation of the simple vehicle) and equation 15 makes it clear that this complex truck will have steady-state turning properties similar to those of a simple vehicle with a wheelbase of ℓ_e and equivalent front and rear tires.

Also, note that T/ℓ^2 and $C_{\alpha r/f}$ are both positive in all practical situations. Thus, the quantity within the brackets in equation 16 is always greater than unity, and, therefore, the equivalent wheelbase of this truck is always longer than the actual wheelbase. Since longer wheelbases result in higher critical velocities (equation 8), multiple, nonsteering axles have a stabilizing influence on the truck.

Equation 16 can also be interpreted to mean that the equivalent wheelbase is composed of three parts: the actual wheelbase, ℓ, plus two additional parts, (T/ℓ) and (T/ℓ) $(C_{\alpha r/f})$. In fact, it can

be shown that these additional parts have very specific physical interpretations as shown in **figure 7**. That is, the multiaxle truck behaves like an *equivalent* two-axle vehicle whose front axle is located the distance (T/ℓ) $(C_{\alpha r}/C_{\alpha f})$ forward of the front axle of the truck and whose rear axle is located the distance (T/ℓ) aft of the center of the rear axle group of the truck. (A limited, but intuitively pleasing proof for this interpretation of equivalent wheelbase is given in **appendix A** of [4].)

The differences between the forms of equation 14 and equation 15 are reflected in the handling diagrams of a multiaxle truck, depending on whether those diagrams are based on path curvature normalized by the wheelbase, ℓ, or by the equivalent wheelbase, ℓ_e. Consider this example: a three-axle truck with dual tires on the two nonsteering, rear axles. The same tire is used at all positions on this vehicle, and these tires are linear ($dF_y/d\alpha$ is constant). The wheelbase of the vehicle is 6 meters and $\Delta_1 = \Delta_2 = 0.6$ meter. Then in equation 14: $\ell = 6$, $T = 0.36$, and $C_{\alpha r}/C_{\alpha f} = 4$. And from equation 16, $\ell_e = 6.5$ m. Consider three cases of this truck, namely, case 1 in which the vehicle's center of gravity is located such that K = 0 deg/g, case 2 in which the center of gravity is moved forward such that K = 3.2 deg/g, and case 3 in which the center of gravity is moved rearward such that K = –3.2 deg/g.

The handling diagrams for these three vehicles which derive from equation 14 (that is, based on the geometric wheelbase, ℓ) are shown in **figure 8**. The diagrams are separated into left and right portions containing V-handling curves and R-handling curves, respectively. From top to bottom, the diagrams progress through the three vehicles from K = 3.2 deg/g to K = –3.2 deg/g. These diagrams have several common qualities regardless of the value of K:

- For each given value of K, the slopes of the R-handling curves are identical, i.e. these slopes are independent of the radius at which the tests are conducted.
- The R-handling curves do not, in general pass through the origin, but tend to that condition as radius increases toward infinity.
- The slopes of the V-handling curves change with velocity, the curves rotating clockwise as velocity increases.
- The slope of the V-handling curve approaches the slope of the R-handling curves as velocity increases toward infinity.

All of these common qualities can be predicted by close examination of equation 14.

Also note that, as indicated by the slopes of the R-handling curves, the three vehicles, from top to bottom, are understeer, neutral steer and oversteer as would be implied by the values of K. Also note that 120 kph is the critical speed of the vehicle for which K= -3.2 deg/g, as indicated by the fact that the 120-kph handling curve overlies the 120-kph V-line.

Figure 9 presents the handling diagrams for precisely the same three cases of this example vehicle, but based on path curvature normalized by the equivalent wheelbase (6.3 m) rather than the actual wheelbase (i.e., based on equation 15). It can be seen from the figure that the seemingly *complex* behavior of the linear, multiaxle truck has collapsed to the form of a *simple* linear vehicle. For each value of K, all of the V-handling curves and all of the R-handling curves have collapsed into a single curve. These three handling curves indicate the same understeer/ oversteer qualities as did the infinite-speed and/or infinite-radius curves of figure 8. Also, the same critical velocity of 120-kph is indicated for the vehicle for which K= -3.2 deg/g.

Comparing analysis with real and simulated vehicle tests

A series of steady-turning tests have been conducted using the three-axle truck pictured in **figure 10**. The second axle of this truck is a drive axle equipped with dual tires and the third axle is nondriving and has only single tires. Starting from the front, the three axle loads during testing were 72,300 N, 113,400 N, and 72,300 N.

This truck was subjected to two series of constant-radius tests, each on a radius of 40-m. In one series, all turns were to the left. In the other, all were to the right. Two series of constant-velocity tests were also conducted, one at 70 kph and one at 90 kph. Only right turns were used in these tests. In general, the test data show the vehicle to be quite linear through 0.4 g.

The test results are presented in **figure 11**. [13] .The figure contains three handling diagrams. Each diagram presents the results from all tests. However, starting from the top, the diagrams are based, respectively, on path curvature normalized by:

- 5.585 m, the geometric wheelbase (i.e. the longitudinal distance from the front axle to the geometric center of the rear axles),

- 5.84 m, the estimated equivalent wheelbase for $a_y = 0$, as calculated using a formula similar to equation 16 and the known tire and vehicle parameters (see the appendix),
- 5.88 m, the equivalent wheelbase for $a_y = 0$, as determined directly from the test-track data.

Examining the top diagram, it can be seen that when the geometric wheelbase is used to develop the handling diagram, the results from the constant-radius tests are clearly offset from the origin as predicted by the simplified theory. (The difference in slopes between the left-turning and right-turning constant-radius tests is believed to result from the asymmetric effect of the steering-system compliances. Also see the discussion on simulation results below.) In the same diagram, the data taken at constant velocities of 70 and 90 kph are nearly the same. The small difference that does appear is opposite of what is expected from the preceding discussion. It is believed that experimental scatter exceeds the complex influence at these velocities. (Again, see the following discussion on simulation results.) Finally, comparing all three of the left-turning handling curves, the constant-radius curve is the most steeply sloped, as the simplified theory would predict for an understeer truck.

In the second handling diagram of figure 11, the equivalent wheelbase estimated from the theory has been used to normalize path curvature. The data from the four separate tests have moved closer to a single curve as expected. However, there remains a small separation between the several handling curves (i.e., at $a_y = 0$, at which equivalent wheelbase was estimated). Apparently there is some small error in the measured parameter values or some applicable qualities of the vehicle have not been included in the analysis.

The equivalent wheelbase of the test vehicle was also found directly from the test data, simply by determining the value of the normalizer of path curvature which produced the “best match” among the several handling curves. By trial and error, this value was found to be 5.88 m. The resulting handling diagram appears at the bottom of figure 11. The handling curves do appear to match slightly better (at $a_y = 0$) in this diagram than in the center diagram, but the difference is small. Note also that, in the second and third diagrams, there is a small offset of the handling curves with respect to the origin. It is believed that this probably results from greater compliance exhibited by the steering system at and near the on-center position.

The data set gathered at the test track was expanded by simulating the same vehicle in a series of constant-velocity tests conducted at 50, 70, and 90 kph, respectively. The simulated tests were conducted in both left- and right-turn directions. The simulations were accomplished using an ADAMS model developed and routinely used by Volvo. This vehicle model is nonlinear and quite complex but does contain one important simplification: each dual-tire pair is represented as a single, lumped tire. This can be expected to result in a slightly shorter equivalent wheelbase for the simulated vehicle than for the real test vehicle. (See the appendix as well as the following discussion.)

Figure 12 presents the handling diagram, based on the geometric wheelbase, of all of the right-turning, constant-velocity tests, i.e., from the test track and from simulation. With the exception of the two points at approximately 0.35 g, these data show a reasonably good match between the data from simulated and actual tests at 70 and 90 kph. The data from simulation clearly show the expected relationship between results from tests conducted at different velocities, as predicted by the simplified theory. That is, as the test velocity increases, there is a progressive rotation of the handling curve in the oversteer direction with an apparently asymptotic approach to a maximum slope at high velocity.

Figure 13 presents all of the results from simulation in a handling diagram based on the geometric wheelbase. In particular, the results from left-turning tests are superimposed on the right-turning results shown previously in. The left-to-right asymmetry seen in the test data (figure 11) is clearly repeated in simulation. More to the point herein, the expected relationship between tests at different velocities is repeated in the left-turning simulations.

Finally, **figure 14** presents all of the results from simulation in a handling diagram in which path curvature has been normalized by the estimated equivalent wheelbase, 5.78 m. (Since the simulation of the vehicle does not include the influence of dual tires, that effect was also left out of the calculation for this estimate of equivalent wheelbase. Thus, the equivalent wheelbase estimated here is slightly less than the value of 5.84 m estimated for the real vehicle.) Since the parameters used to define the vehicle in simulation were closely related to those used to estimate equivalent wheelbase, it is not surprising that this estimated value also appears to produce the best match among the several handling curves. That is, all of the separate handling curves have collapsed to virtually a single curve at low levels of lateral accelerations. At higher levels, the right-to-left asymmetry is still apparent, but the right- and left-turn handling curves remain very well matched, respectively.

Summary

The classic analyses of the steady-state turning of the motor vehicle are based on a model of a *simple vehicle* for which it is assumed that lateral acceleration is the only motion variable on which front and rear slip angles depend [1,2,3]. This paper examined the behavior of a more *complex vehicle* for which tire slip angles depend on lateral acceleration plus another motion variable [4]. The handling diagram was used as an aid in explaining the behavior of both simple and complex vehicles.

The criterion for stability in a steady turn remains the same for the complex vehicle as it has been understood for the simple vehicle, but the notions of neutral steer and the related properties of understeer and oversteer are altered. However, the steady-turning of the complex vehicle is similar to that of a simple vehicle with an equivalent wheelbase, ℓ_e. From these observations, it is argued that it is appropriate to refer to the quantity $d(\delta - \ell_e/R)/da_y|_{V=V_c}$ as the stability gradient and to the quantity $d(\delta - \ell_e/R)/da_y|_{R=R_c}$ as the understeer gradient.

The commercial truck with multiple, nonsteering rear axles is an example of the complex vehicle. The turning behavior of a multiaxle truck with linear tires was analyzed and an expression for its equivalent wheelbase was determined. A numerical example was presented as an aid to explaining the analysis.

Finally, steady-state turning tests were conducted on a real truck. Results from track testing were extended through simulation using an ADAMS vehicle model. Results from both testing and simulation substantially confirm the findings of the simplified analysis.

Introduction Content

REFERENCES

1. Pacejka, H. B. “Simplified analysis of steady-state turning behaviour of motor vehicles. Part 1. Handling diagrams of simple systems” *Vehicle Systems Dynamics* 2. 1973. pp. 161-172.

2. Pacejka, H. B. “Simplified analysis of steady-state turning behaviour of motor vehicles. Part 2. Stability of the steady-state turn” *Vehicle Systems Dynamics* 2, 1973, pp. 173-183.

3. Pacejka, H. B. “Simplified analysis of steady-state turning behaviour of motor vehicles. Part 3. More elaborate systems.” *Vehicle Systems Dynamics* 2, 1973, pp. 184-204.

4. Winkler, C.B. “Simplified analysis of the steady-state turning of complex vehicles.” Accepted for publication in *Vehicle Systems Dynamics* 29, 1998.

5. *Vehicle dynamics terminology*. SAE J670e, Society of Automotive Engineers, Warrendale, Pa, 1978, 21 p.

6. *Road vehicles—vehicle dynamics and road holding—vocabulary*. International Standard ISO 8855: 1991 (E/F), International Organization for Standardization, Geneva, 1991, 28 p.

7. Winkler, C.B., Fancher, P.S., and MacAdam, C.C. *Parametric analysis of heavy duty truck dynamic stability*. Report number UMTRI-83-13, University of Michigan Transportation Research Institute, Ann Arbor, 1983, 170 p.

8. MacAdam, C.C. *A computer-based study of the yaw/roll stability of heavy trucks characterized by high centers of gravity*. SAE paper number 821260, Society of Automotive Engineers, Warrendale, Pa, 1982, 22 p.

9. Fancher, P.S. and Mathew, A. *A vehicle dynamics handbook for single-unit and articulated heavy trucks*. Report number UMTRI-86-37, University of Michigan Transportation Research Institute, Ann Arbor, 1987, 367 p.

10. Gillespie, T. D. and Winkler, C. B. “On the directional response characteristics of heavy vehicles.” *The Dynamics of Vehicles on Roads and Tracks*, 1978, pp. 165-187.

11. Bundorf, R.T. and Leffert, R.L. *The cornering compliance concept for description of directional control properties*. SAE paper number 760713, Society of Automotive Engineers, Warrendale, Pa, 1976, 14 p.

Introduction Content

APPENDIX–ESTIMATING THE EQUIVALENT WHEELBASE OF THE TEST VEHICLE

Equation 16 is overly simplified for estimating the equivalent wheelbase of a real vehicle. This is especially true for the test vehicle since it (1) used different tires on its three axles, (2) did not have equal loading on the two rear axles, and (3) used dual tires on the second axle. A more adequate expression appears as equation 13 of [10], and is repeated here:

$$\ell_e = \ell\left\{1+\frac{\Delta^2}{\ell^2}\left[\frac{1+\dfrac{4C_{\alpha2}C_{\alpha3}}{C_{\alpha1}(C_{\alpha2}+C_{\alpha3})}-\dfrac{\ell}{\Delta}\dfrac{C_{\alpha2}-C_{\alpha3}}{C_{\alpha2}+C_{\alpha3}}+\dfrac{D^2}{\Delta^2}\dfrac{C_{s2}+C_{s3}}{C_{\alpha2}+C_{\alpha3}}\left(1+\dfrac{C_{\alpha2}+C_{\alpha3}}{C_{\alpha1}}\right)}{1-\dfrac{\Delta}{\ell}\dfrac{C_{\alpha2}-C_{\alpha3}}{C_{\alpha2}+C_{\alpha3}}}\right]\right\}, \quad \text{(A)}$$

where $\Delta = \Delta_1 = \Delta_2$,

and

$C_{\alpha i}$ i = 1,2,3, are the sums of the cornering stiffnesses of all tires on the first, second, and third axles, respectively, and

C_{si} i = 2,3, are the sums of the longitudinal stiffnesses of all the dual tires on the second and third axles, respectively.

Equation A (as well as all of the equations in this paper) acknowledges only the influence of the tires while ignoring the understeer/oversteer qualities of the suspensions and steering system. The cornering-compliance concept has been used to lump these latter qualities with the tire compliances to produce equivalent cornering stiffnesses which were then used in equation A [11]. These equivalent compliances (evaluated at $a_y = 0$) and the other vehicle parameters required by equation A appear in table A. These values yield equivalent wheelbases of 5.84 m for the real test vehicle (including the influence of dual tires on the second axle) and 5.78 m for the simulated test vehicle (without the influence of dual tires).

Table A. Test vehicle parameters

Equivalent tire cornering stiffness, kN/rad†		
$C_{\alpha1}$	$C_{\alpha2}$	$C_{\alpha3}$
-326	-798	-451

C_{s2}: -737 kN (real test vehicle)††
C_{s2}: 0 (simulated test vehicle)
C_{s3}: 0
D: 0.330 m
Δ: 0.685 m
ℓ: 5.585 m

† Includes the influences of tire compliances and of suspension and steering-system kinematics and compliances.

†† This parameter was not from the tires of the test vehicle but was estimated from measurements of a similar drive-axle tire.

Introduction Content

FOOTNOTES

1 This work is the province of working group 6 for heavy vehicles (WG6) of subcommittee 9 for vehicle dynamics and road holding (SC9) of technical committee 22 for road vehicles (TC22) of the ISO. Mr. Aurell is the convenor of WG6, and Mr. Winkler is one of its expert members.

Return to paper

2 Numbers in brackets refer to the bibliographic references given at the end of this paper.

Return to paper

3 The substitution of lateral acceleration for centripetal acceleration, as in equation 1, will be used throughout this paper, as much for brevity of notation as for any other reason. Note that this is valid

4 Lateral acceleration (a_y) is expressed in gravitational units throughout this paper.

Return to paper

5 SAE coordinate systems and sign conventions are used in all of the figures and equations in this paper [5].

Return to paper

6 In later sections, trucks with many rear tires will be considered, and these definitions will still apply

Return to paper

7 More precisely, both the SAE and ISO use the *steering-wheel-angle gradient divided by the overall steering ratio* rather than the gradient of the front-wheel steer angle, δ, in their definitions [5,6]. For the simplified models in this paper, which do not consider suspension and steering-system effects, these are the same. Later, when considering test and simulation data, the more complete definition is applied. Also, SAE refers to the ratio ℓ/R as the Ackerman angle and ISO refers to it as the dynamic reference angle [5,6]. Herein, this quantity is called normalized path curvature.

8 SAE presents its definition as the full derivative "…at a given trim and test condition." The ISO definition is couched in terms of partial derivatives but without comment on other independent variable(s).

Return to paper

9 More precisely, Pacejka showed that stable turning requires $\phi_f\ \phi_r\ \partial\delta/\partial\ell/R > 0$. Since ϕ_f and ϕ_r are of the same sign in virtually all practical operating conditions, they are often dropped from the expression for the stability criterion, as is done herein.

Return to paper

10 In order to enhance the points to be made, this handling diagram is for a vehicle with very strong complex and nonlinear effects. A heavily loaded commercial truck with several nonsteering axles and strong nonlinear qualities can exhibit effects of similar strength. Nevertheless, the reader should think of this handling diagram as a generic example.

Return to paper

11 All of Pacejka's equations of section 7 of part 2 hold for the complex vehicle with only the most minor change required in equation 24 [2]. That is, Pacejka's equation 24 becomes $f_i = (dF_i/da_i)|_{a_i=a_{iss},\ u}$ implying that f_i is a function of both slip angle and forward velocity.

Return to paper

12 In figure 4, the stability boundary is shown in the a_y versus $(d - l/R)$ space of the handling diagram, i.e., in relation to the handling curves. Pacejka showed the stability boundary for the nonlinear simple vehicle in the a_y versus l/R space, i.e., in relation to the V- and l/R-lines [2]. The boundary between stable and unstable operating regions for the multiaxle truck have been shown by others on the V versus a_y plane [7,8,9].

Return to paper

13 Note that on the abscissas of figure 11, as well as in the figures to follow, front wheel steer angle, δ, has been replaced by δ_h/N, the measured steering-wheel angle divided by the overall steering ratio. Results are very sensitive to N. The variable steering ratio of the test truck has been accounted for in figure 11. Also see footnote 7.

Return to paper

Content

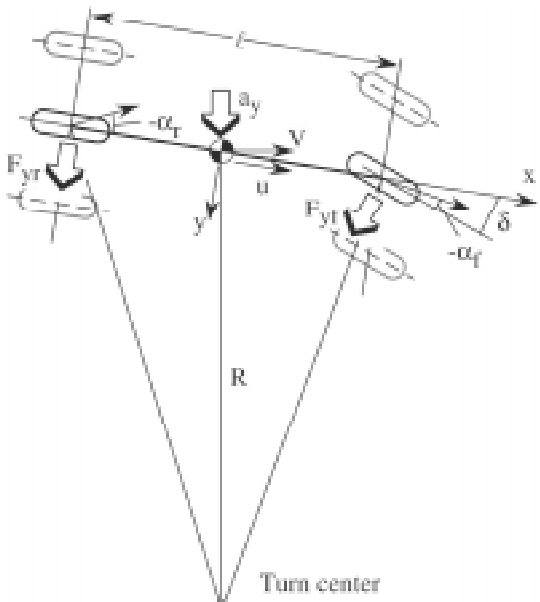

Fig. 1. Simplified model of a simple vehicle in a steady turn

Return to paper

Content

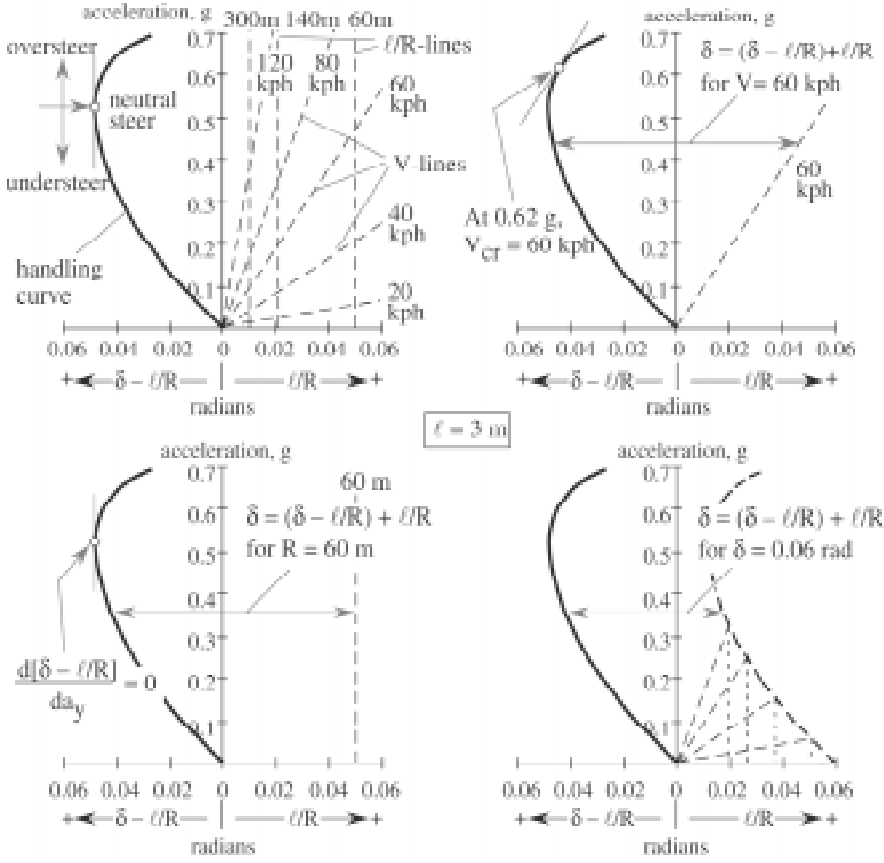

Fig. 2. Handling diagrams for a nonlinear, simple vehicle

Return to paper

Content

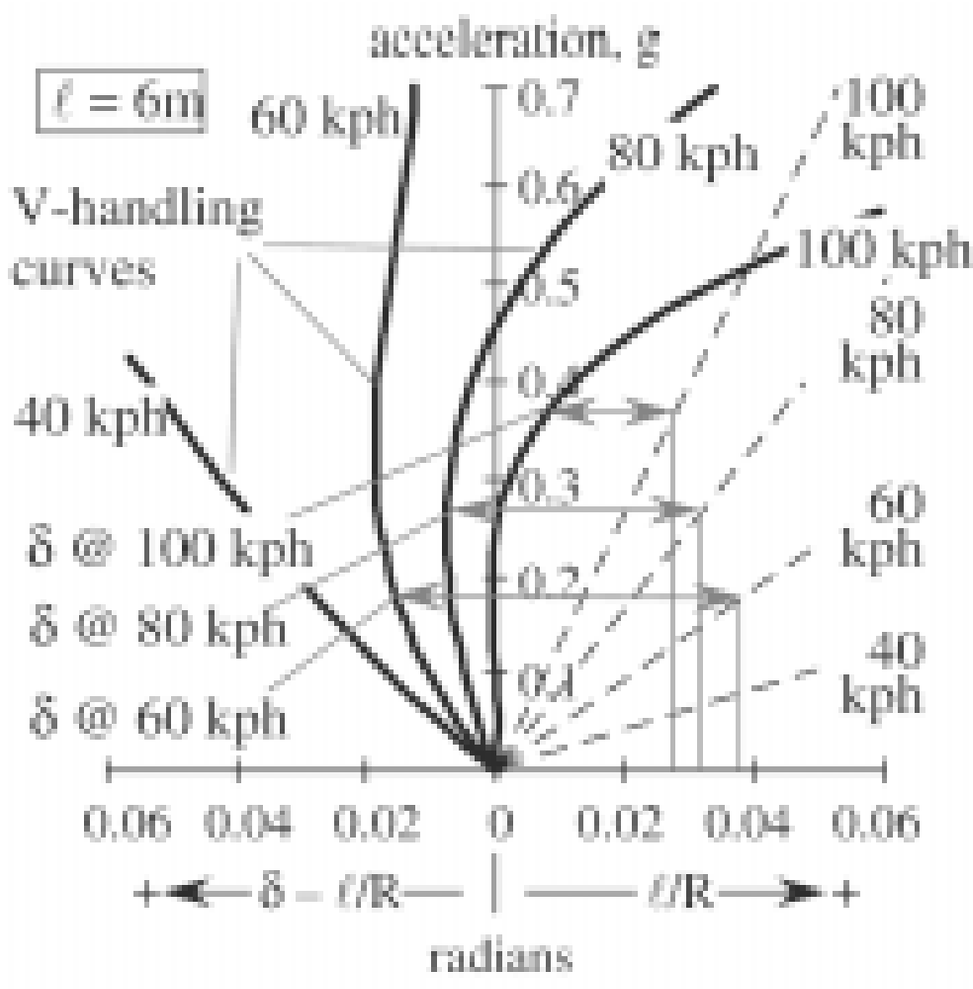

Fig. 3. V-handling diagram for a nonlinear, complex vehicle

Return to paper

Content

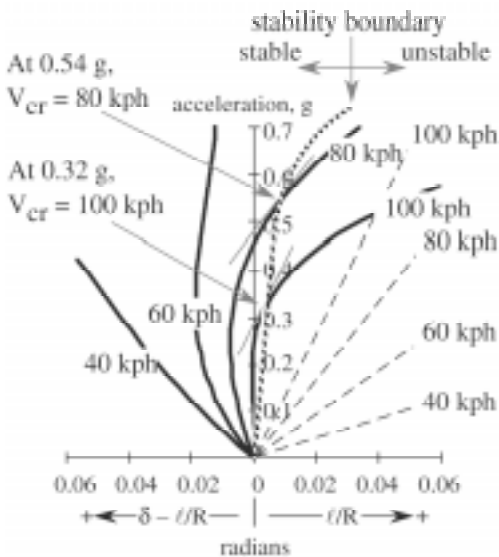

Fig. 4. Slopes of the V-handling curves indicate the critical velocities and the stability boundary for the complex vehicle

Return to paper

Content

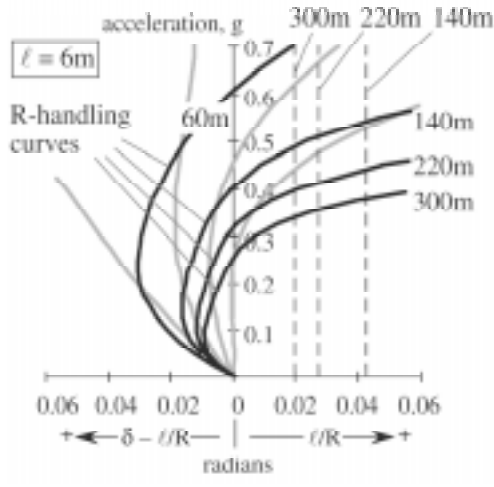

Fig. 5. R-handling curves superimposed on the V-handling curves of a nonlinear, complex vehicle

Return to paper

Content

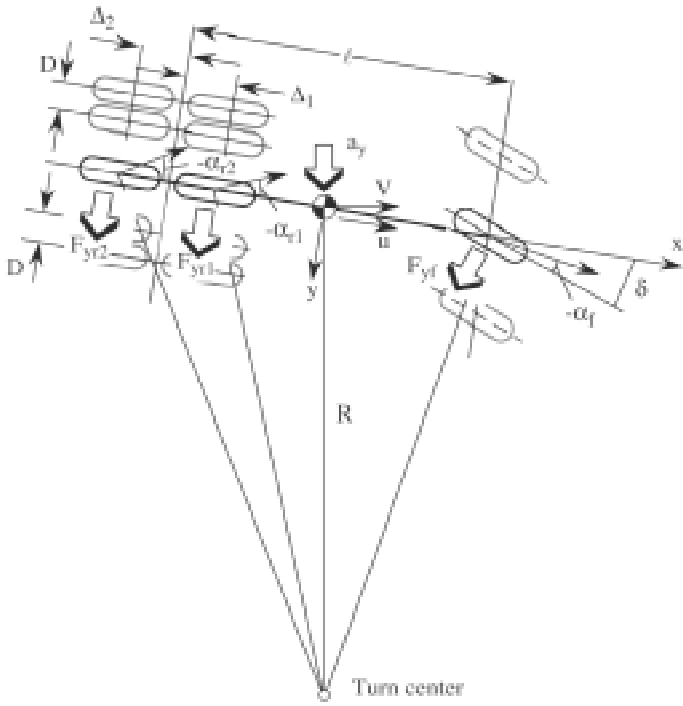

Fig. 6. Simplified model of the three-axle truck in a steady turn

Return to paper

Content

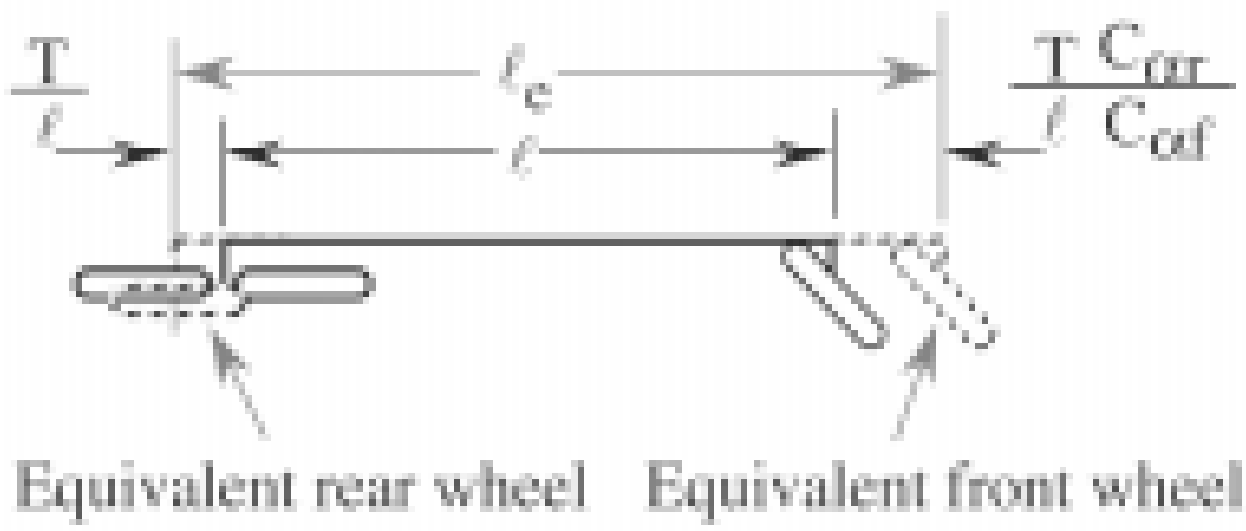

Fig. 7. Physical interpretation of the equivalent wheelbase of a three-axle truck

Return to paper

Content

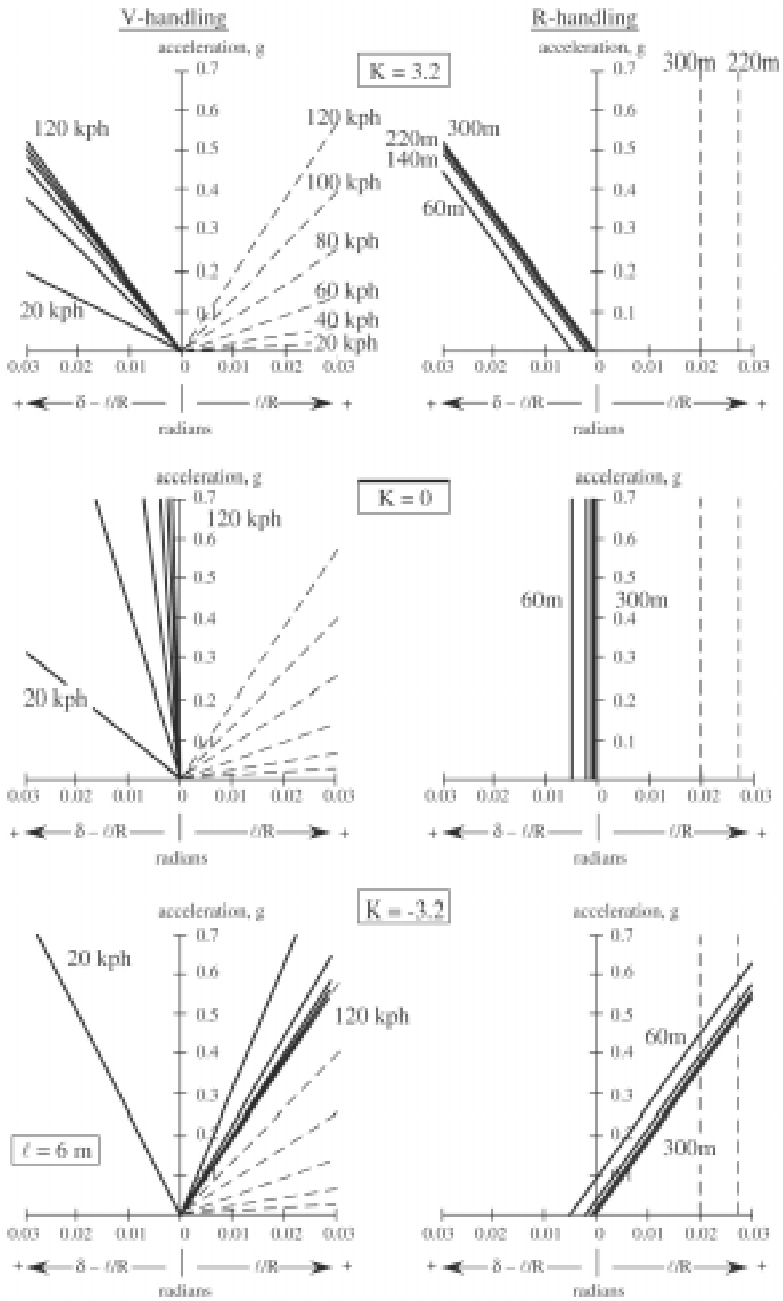

Fig. 8. Handling diagrams for a linear, three-axle truck

Return to paper

Content

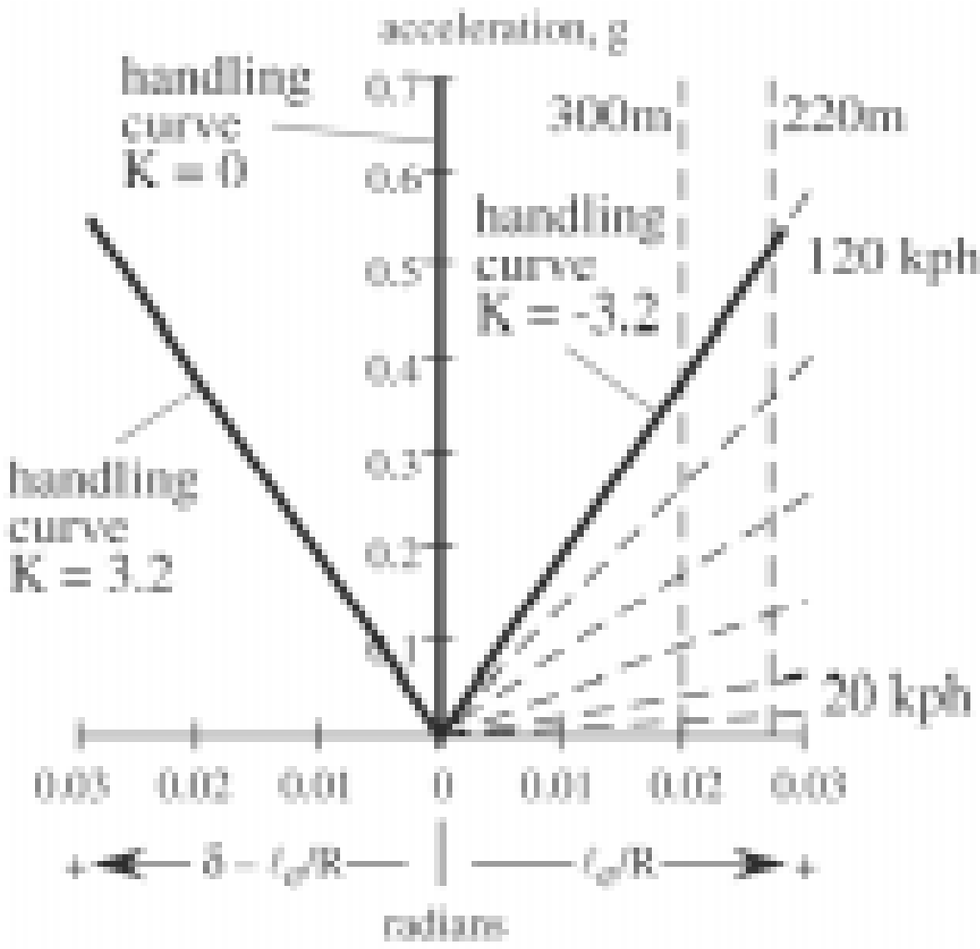

Fig. 9. Handling diagrams for a linear, three-axle truck based on the equivalent wheelbase

Return to paper

Content

Fig. 10. The test vehicle

Return to paper

Content

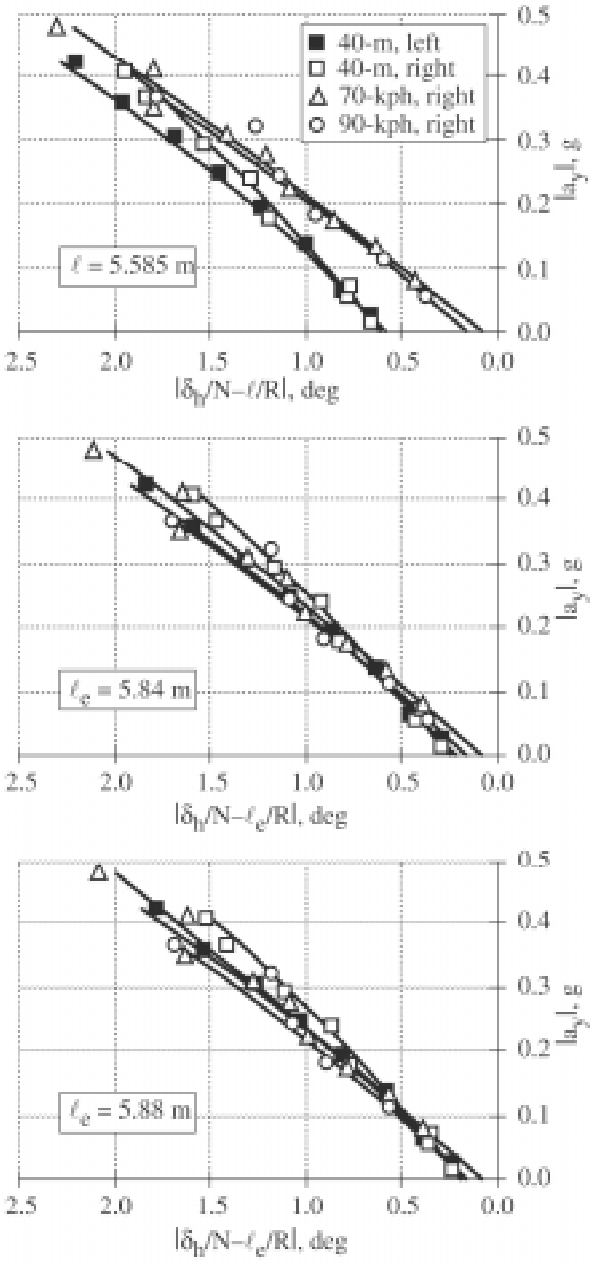

Fig. 11. Handling diagrams derived from test-track data

Return to paper

Content

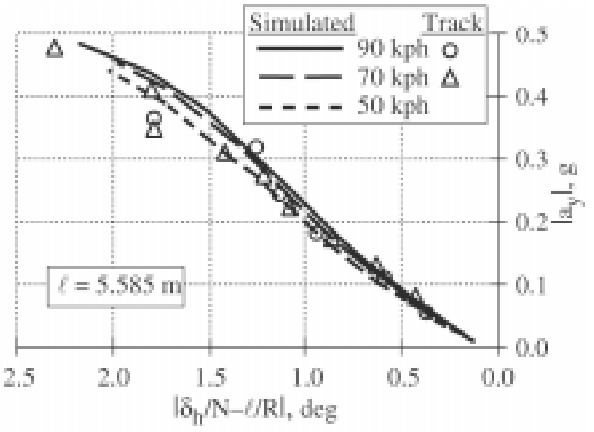

Fig. 12. Simulated and actual right-turning, constant-velocity tests

Return to paper

Content

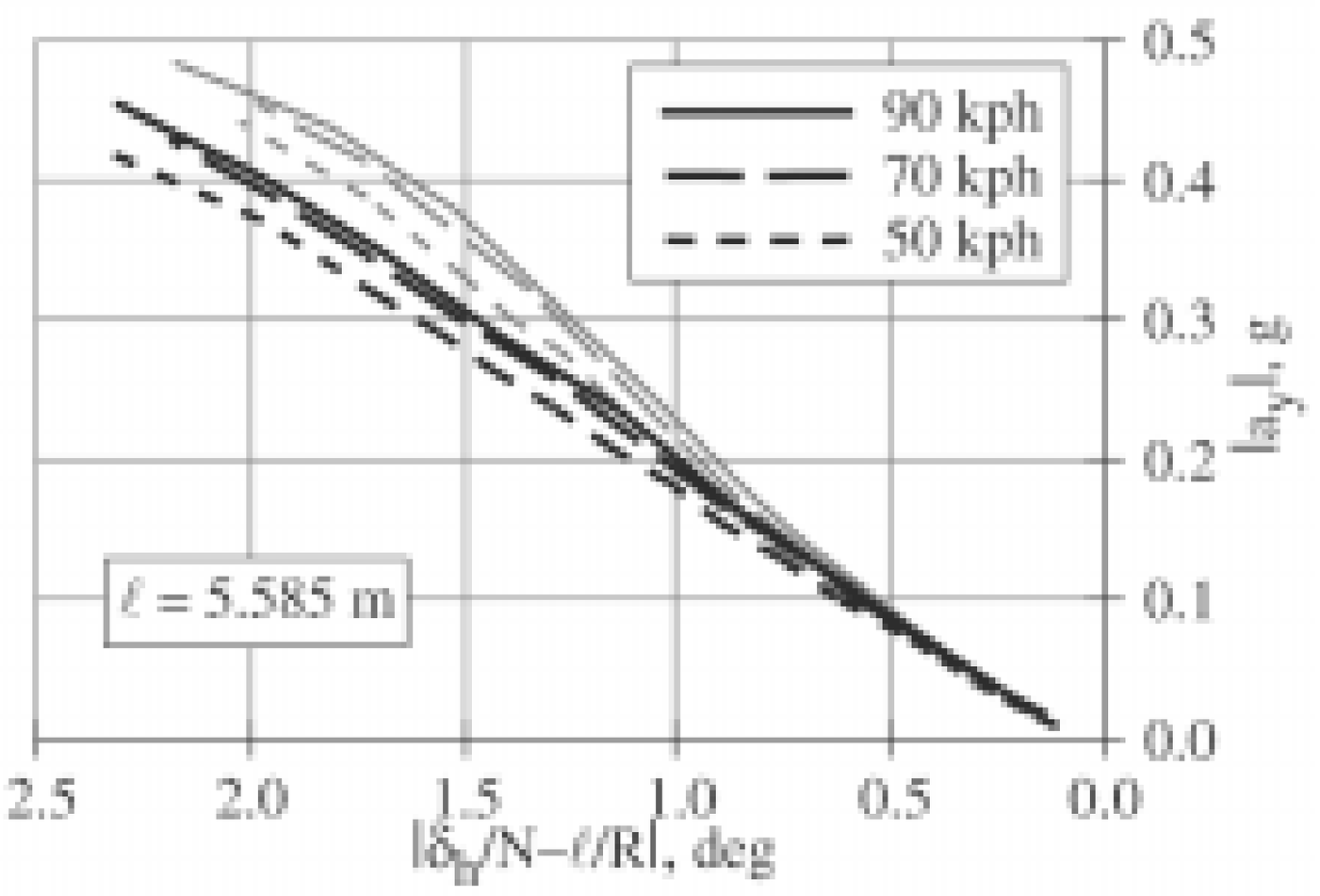

Fig 13. Left-turning simulation results superimposed on right-turning simulation results

Return to paper

Content

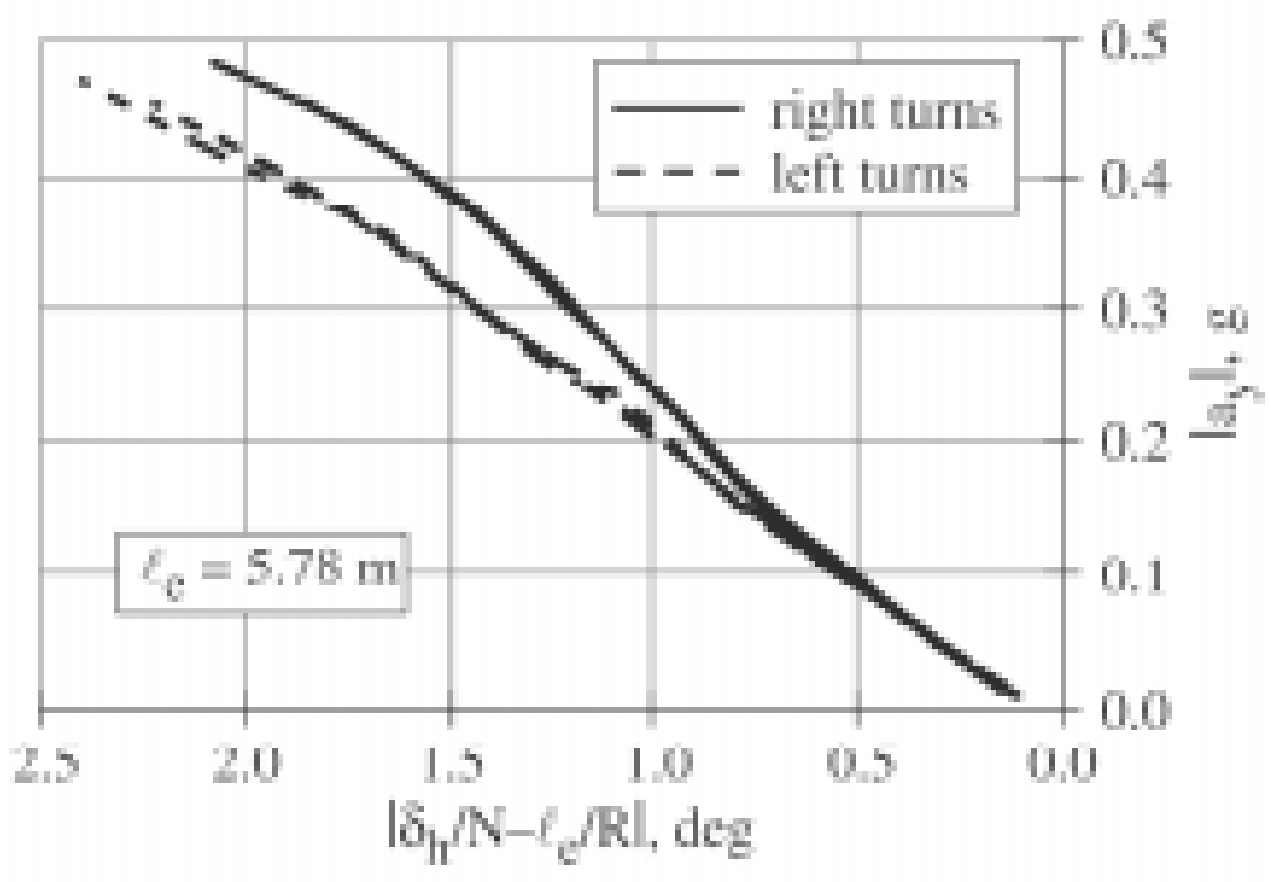

Fig. 14. Handling diagram for all simulation results based on the equivalent wheelbase

Return to paper

Content